

Received May 13, 2021, accepted May 31, 2021, date of publication June 11, 2021, date of current version June 23, 2021.

Digital Object Identifier 10.1109/ACCESS.2021.3088439

# Satellite On-Orbit Anomaly Detection Method Based on a Dynamic Threshold and Causality Pruning

SIYA CHEN<sup>1</sup>, JIN G.<sup>1</sup>, AND XINYU MA<sup>2</sup>

<sup>1</sup>College of Systems Engineering, National University of Defense Technology, Changsha 410073, China

<sup>2</sup>Beijing Aerospace Control Center, Beijing 100048, China

Corresponding author: Jin G. (jinguang@nudt.edu.cn)


**ABSTRACT** It is difficult for existing deep learning-based satellite on-orbit anomaly detection methods to define the residual-based detection threshold and identify false anomalies. To solve the above problems, this paper proposes both a detection threshold determination and dynamic correction method and a causality-based false anomaly identification and pruning method. We use the GRU (Gated Recurrent Unit) to model and predict the telemetry parameters to obtain the residual vector; determine and dynamically correct the threshold according to the prescribed false positive rate; propose an improved multivariate transfer entropy method to identify the causal relationships between the telemetry parameters; and, based on the causality, determine whether the detected parameter anomalies are false. Experiments show that the precision, recall, and F1-score of the method proposed in this paper are superior to the current typical method, and the false positive rate is significantly reduced, demonstrating the effectiveness of the proposed method.

**INDEX TERMS** Dynamic threshold, causality pruning, anomaly detection, GRU, on-orbit satellite.

## I. INTRODUCTION

Domestic and foreign aerospace practices show that regardless of how strict the measures that are taken in the development stage are, on-orbit satellite failures are unavoidable. On-orbit satellites are affected by their working environment and their own conditions, and anomalies often occur in various subsystems or devices. Telemetry data come from the real-time state of a satellite collected by various sensors, which is a true reflection of the satellite's working state. The processing and analysis of telemetry data are effective means for monitoring the state of satellites and for carrying out the long-term management of on-orbit satellites [27].

Anomaly detection (AD) is a vast area of research given its diverse applications [13], [34]. The fixed threshold method is currently the most commonly used satellite anomaly detection method in engineering [37], but due to the large number of telemetry parameters and the influences of unknown factors such as the space environment, it is difficult to set an appropriate threshold for each parameter, and it is difficult to guarantee the rationality of the detection threshold [38]. Anomaly detection based on expert experience [2], [24], [36]

The associate editor coordinating the review of this manuscript and approving it for publication was Dazhong Ma .

can target only known anomalies or faults. Due to the complexity of the satellite system and the changeable operating environment, unexpected failures often occur, and they are difficult to detect based on expert experience.

In recent years, with the accumulation of spacecraft telemetry data and the continuous development of data mining technology, data-driven spacecraft anomaly detection methods have become a research hotspot [14], [17], [26], [35].

Song *et al.* [31] proposed an improved GNG method based on incremental learning for online anomaly detection. Pilastre *et al.* [28] proposed an anomaly detection method based on sparse representation and dictionary learning for discrete data and continuous data. Nachman *et al.* [23] proposed a new unsupervised density estimation (ANODE) technique for anomaly detection. Although these methods have achieved good results in the detection of satellite on-orbit anomalies, when these methods define the detection threshold, they are all defined based on manual experience. This sometimes causes the threshold to be unreasonably determined, causing a large number of misjudgements or missed judgements.

In addition to the definition of the threshold, the pruning of false anomalies is another problem to be solved. In anomaly detection, few references consider anomaly pruning.

Hundman *et al.* [15] proposed the use of LSTM and non-parametric thresholds for spacecraft anomaly detection and proposed an anomaly pruning method. [32], [37] also used these methods for anomaly pruning. However, the pruning methods were judged only from the perspective of the parameters themselves and did not consider the correlation between the telemetry parameters.

In addition, due to the large amount of telemetry data, an ordinary satellite may generate 85 TB of data per day [15], and the training of existing data-driven models is very time-consuming.

To solve the above problems of data-driven methods, this paper proposes a satellite on-orbit anomaly detection method based on a dynamic threshold and causality pruning. First, a single-channel GRU model is used to predict the telemetry parameters, and the residual vector is obtained. According to the predicted residual, a method for determining and correcting the threshold according to the false alarm rate is proposed. In order to reduce false anomalies, an improved multivariate transfer entropy method is proposed to identify the causal relationships between telemetry parameters and prune false anomalies according to causality, effectively reducing the false positive rate. Experiments show that compared with other methods, the method proposed in this paper achieves a higher precision, recall, and F1-score, which verifies the effectiveness of this method.

The contributions of this paper are as follows:

- 1) This paper proposes an improved multivariate transfer entropy method to judge the causal relationships between the telemetry parameters in a satellite system. The main improvement to the original model is reflected in the judgement of causality.
- 2) This paper proposes a method to dynamically define the threshold based on the prediction residuals.
- 3) This paper proposes an anomaly pruning method based on the causal relationships between telemetry parameters.
- 4) Combining the above methods, this paper proposes a satellite on-orbit anomaly detection method based on a dynamic threshold and causality pruning.

The structure of the remainder of this paper is as follows. Section I is the introduction, which describes the status of satellite on-orbit anomaly detection research and analyses the problems of satellite on-orbit anomaly detection methods. Section II introduces the framework of the algorithm in this paper. Section III proposes an improved multivariate transfer entropy method to identify the causal relationship between telemetry parameters. Section IV introduces the satellite on-orbit anomaly detection method based on a dynamic threshold and the causality pruning method in detail. Section V uses actual telemetry data to verify the method proposed in this paper. Section VI summarizes the method proposed in this paper and proposes issues that need further research.

## II. SATELLITE ON-ORBIT ANOMALY DETECTION METHOD BASED ON A DYNAMIC THRESHOLD AND CAUSALITY PRUNING

The satellite on-orbit anomaly detection method proposed in this paper is shown in Fig.1. The whole method is divided into two parts: offline and online. The GRU modelling and detection threshold determination, causality identification and causality pruning rules are included in the offline execution part; the detection threshold correction, online anomaly detection, and causal pruning components are included in the online execution part.

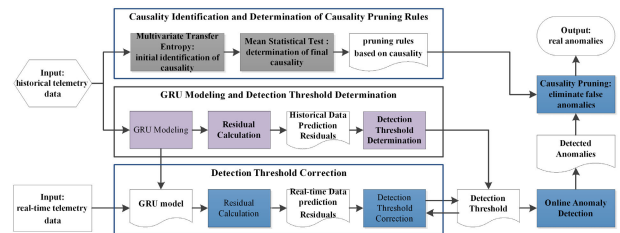


FIGURE 1. Satellite on-orbit anomaly detection framework.

This paper uses the GRU to model and predict telemetry parameters. The GRU (Gated Recurrent Unit) [5] is a kind of Recurrent Neural Network (RNN), like LSTM (Long Short-Term Memory) [12]; the GRU has also been proposed to solve the problems of long-term memory and gradients in back propagation. Compared with LSTM, the GRU model is simpler and has the same predictive ability and higher computational efficiency, which is conducive to building a larger model [4]. When the algorithm is offline, a single-channel GRU model is established for each telemetry parameter, and the established GRU model is used to predict the telemetry data offline and online. After the residual vector of the offline prediction is obtained, the initial detection threshold is determined according to the method of automatically defining the threshold proposed in this paper. After the residuals of the online prediction are obtained, the current threshold is corrected using the method proposed in this paper, and online anomaly detection is performed according to the corrected threshold. For states above the threshold, they are initially marked as abnormal. Then, causality pruning is used to further judge them, and the abnormalities after pruning are the real anomalies.

## III. CAUSALITY IDENTIFICATION

### A. RELATED WORK

Causality modelling is currently a difficult problem in the field of data modelling and machine learning. At present, the most commonly used causality modelling method is the Granger causality model [9], [16]. However, the classic Granger causality model is linear and is not suitable for nonlinear models. [3], [8] improved this method and proposed a nonlinear Granger causality model. However, these models are designed for specific scenarios, and deviations from the assumptions will lead to false causality.

Schreiber [29] proposed the transfer entropy method based on information theory to identify the causality between parameters. Compared with the Granger causality model, transfer entropy is applicable to linear or nonlinear systems, and there is no need to make specific assumptions about the causality between parameters. In addition, the causality based on the transfer entropy is not symmetrical and therefore more reasonable. Since transfer entropy was proposed, it has been applied to many fields, such as economy [22], biology [33], and fault propagation [20].

Although many methods for identifying the causality between parameters based on classic transfer entropy have been proposed, there are still many problems. First, the existing methods use a one-to-one approach to determine the causal relationships between parameters, which is not only complicated to calculate but also causes redundant causal relationships. Second, it is assumed that the causal relationship between two parameters, such as  $\alpha$  and  $\beta$ , are being judged. If the transfer entropy of  $\alpha$  to  $\beta$  is greater than the transfer entropy of  $\beta$  to  $\alpha$ , then  $\alpha$  is the cause of  $\beta$ . This discrimination method is actually illogical, especially when the transfer entropy of  $\alpha$  to  $\beta$  is not much different from the transfer entropy of  $\beta$  to  $\alpha$ . This discrimination method will cause false causality.

In order to solve the above problems, this paper draws inspiration from multivariate transfer entropy theory proposed by Lizie *et al.* [21] and proposes an improved multivariate transfer entropy method to identify the causal relationships between high-dimensional telemetry parameters.

## B. CAUSALITY IDENTIFICATION BASED ON IMPROVED MULTIVARIATE TRANSFER ENTROPY

Transfer entropy is a nonparametric method proposed by Schreiber [29] to measure the directed information flow in a random process.

Let  $X = (x_n, n = 1, 2, \dots, N)$  and  $Y = (y_n, n = 1, 2, \dots, N)$  be two random processes,  $X$  be a Markov process of order  $k$ , and  $Y$  be a Markov process of order  $l$ , namely:

$$p(x_{n+1} | x_n, \dots, x_1) = p(x_{n+1} | x_n^{(k)}) \quad (1)$$

$$p(y_{n+1} | y_n, \dots, y_1) = p(y_{n+1} | y_n^{(l)}) \quad (2)$$

$$x_n^{(k)} = (x_n, x_{n-1}, \dots, x_{n-k+1})$$

$$y_n^{(l)} = (y_n, y_{n-1}, \dots, y_{n-l+1})$$

The transfer entropy is defined as:

$$T_{Y \rightarrow X}(k, l) = \sum p(x_{n+1}, x_n^{(k)}, y_n^{(l)}) \log \frac{p(x_{n+1} | x_n^{(k)}, y_n^{(l)})}{p(x_{n+1} | x_n^{(k)})} \quad (3)$$

$$T_{X \rightarrow Y}(k, l) = \sum p(y_{n+1}, x_n^{(k)}, y_n^{(l)}) \log \frac{p(y_{n+1} | x_n^{(k)}, y_n^{(l)})}{p(y_{n+1} | y_n^{(l)})} \quad (4)$$

Lizie *et al.* [21] proposed multivariate transfer entropy to find the causal parameter of each parameter in the system. Assuming that the parameter set in the system is  $\mathbf{D}$ , there are three main steps in multivariate entropy transfer:

- 1) Initialize the causal parameter set  $V_X$  of a specific parameter to an empty set.
- 2) For each parameter in  $D \setminus V_X$ , calculate the amount of information they contribute to  $X$ , find the parameter  $Z$  that contributes the most information, and judge whether it passes the maximum statistical test [25]. If the parameter passes the test, add this parameter to  $V_X$  and repeat this step until  $D \setminus V_X$  is an empty set or the maximum contribution information [25] fails the maximum statistical test.
- 3) Prune  $V_X$ . That is, use the minimum statistical test [25] to test and delete redundant variables in  $V_X$ .

An obvious problem with the above-mentioned multivariate entropy transfer method is the misjudgment of causality. In multivariate transfer entropy, as long as the information provided by the variable  $Z$  to  $X$  is significant (that is, for  $\forall Z \in V_X$ ,  $T_{Z \rightarrow X | V_X \setminus Z}$  is significant [25]),  $Z$  is added to the set of causal parameters  $V_X$ . This leads to a problem: if  $T_{Z \rightarrow X}$  is significant and  $T_{X \rightarrow Z}$  is also significant, then  $X$  and  $Z$  are causally related to each other, which is illogical. From the perspective of information flow, if one parameter is the causal parameter of another parameter, then the amount of information it contributes to this parameter is much greater than the amount of information that this parameter contributes to it. This difference in the information contribution is reflected in the difference in the transfer entropy, and the difference in the transfer entropy is called the directional transfer entropy (DTE). In order to judge whether the difference in the DTE is significant, this paper proposes a mean statistical test method to judge whether the directional transfer entropy between two parameters is significant so as to judge whether there is a causal relationship between the two parameters and the direction of the causal relationship. The definition of directional transfer entropy is shown in (5):

$$TE_{Z \rightarrow X} = T_{Z \rightarrow X} - T_{X \rightarrow Z} \quad (5)$$

Assuming that test  $Z$  is the causal parameter of  $X$ , calculate  $TE_{Z \rightarrow X}$ . If  $TE_{Z \rightarrow X}$  is less than zero, then  $Z$  is not the causal parameter of  $X$ . If  $TE_{Z \rightarrow X}$  is nonzero, perform a mean statistical test to judge whether  $TE_{Z \rightarrow X}$  is significant.

Assuming that the initial causal parameter set of parameter  $X$  that is obtained when using the multivariate transfer entropy method is  $\mathbf{C}$ , the steps of the mean statistical test are as follows:

- 1) For each variable  $c \in \mathbf{C}$ , For each variable  $c \in \mathbf{C}$ , represents the candidate set of the dependent variable;  $S$  surrogate time series  $C'_{j,1}, \dots, C'_{j,S}$  are generated; and the corresponding transfer entropy differences  $TE_{C'_{j,1} \rightarrow X}, TE_{C'_{j,2} \rightarrow X}, \dots, TE_{C'_{j,S} \rightarrow X}$  are calculated. The number of  $S$  must be greater than or equal to  $1/\alpha_{\max}$ , where  $\alpha_{\max}$  represents the significance level.

- 2) Among all candidate causal variables, calculate the following for each surrogate time series:  $TE_s^* := \text{mean}(TE_{1,s}, TE_{2,s}, \dots, TE_{n,s})$ , where  $n$  represents the number of candidate dependent variables, which is also the number of comparisons. The obtained  $TE_1^*, TE_2^*, \dots, TE_s^*$  represent the distribution of the mean statistical value.
- 3) Calculate the  $p$ -value of  $T_{Z \rightarrow X}$  as the score greater than the surrogate mean statistical value of  $T_{Z \rightarrow X}$ .
- 4) If the  $p$ -value is less than  $\alpha_{\max}$ , then  $T_{Z \rightarrow X}$  is significant.

The mean statistical test shows that only when  $T_{Z \rightarrow X}$  is larger than  $T_{X \rightarrow Z}$  can the variable  $Z$  be regarded as the causal parameter of  $X$  in a system.

Combining the original multivariate transfer entropy method and the mean statistical test, an improved multivariate transfer entropy algorithm is proposed. Experiments show that the improved multivariate transfer entropy method can effectively identify the true causality between telemetry parameters.

#### IV. THRESHOLD DETERMINATION AND CAUSALITY PRUNING METHOD

##### A. RELATED WORK

In the existing time series anomaly detection methods, it is ultimately necessary to define a threshold, that is, to obtain an anomaly index. If the anomaly index is higher than the threshold, it is judged as an anomaly. Therefore, the selection of the threshold is a particularly important step in anomaly detection. At present, there are three main methods for defining the detection threshold. One method is to define the threshold based on experience [6], [10], [19], [28], [31], [39]. This method is the most widely used. In essence, this kind of method artificially defines a threshold and then calculates the anomaly score through various methods. Once the anomaly score exceeds the threshold, it is marked as an anomaly. The main disadvantage of this method is that the threshold needs to be artificially defined. The defined threshold is very subjective and cannot be changed as the data change. The second method is to assume that the data obey a special distribution, such as a Gaussian distribution. Once it is found that the detected data do not follow this distribution, they are judged as abnormal [1], [7], [18]; however, this method is not practical. In reality, time series data are high-dimensional, unstable, and heterogeneous, and it is unrealistic to assume that the data obey a special distribution. The third method is to automatically define the threshold. [30] proposed the SPOT and DSPOT methods to automatically define the threshold according to Extreme Value Theory [11], but this method is difficult to solve, the calculation is unstable, and it is sometimes impossible to obtain a suitable threshold. [15] proposed a nonparametric method for dynamically defining thresholds, but this method requires artificially setting the initial threshold range. If the initial threshold is unreasonable, the final detection threshold will also be unreasonable, causing many false positives or underreporting.

In order to solve the above problems of threshold definition, this paper proposes a method to automatically define the threshold. In this method, only the range of false alarm rates is required to obtain the appropriate threshold. Compared with other methods, this method is simple to calculate, there is no need to have any prior knowledge about the data, and the threshold can also change as the false alarm rate changes.

##### B. THRESHOLD DETERMINATION AND CORRECTION BASED ON THE FALSE ALARM RATE

The detection threshold is automatically defined according to the residual vector  $\mathbf{e}$  predicted by the GRU. This method is simple to calculate, the threshold can be obtained by only giving the false alarm rate, and the threshold can be modified according to the detection situation. The steps of the method of automatically defining the threshold based on the false alarm rate are as follows:

- 1) Assume that the acceptable false alarm rate range is  $P_1 \sim P_2$ . That is, within each sliding window  $T$ , the false alarm rate is required to be between  $P_1 \sim P_2$ . Using the obtained residual vector  $\mathbf{e}$ , (6) is calculated.

$$P_1 \leq P(e < \epsilon) \leq P_2 \quad (6)$$

From this, the value range of the final threshold  $\epsilon$  can be obtained as  $\epsilon \in [\epsilon_1, \epsilon_2]$ .

- 2) After obtaining the threshold value range, select a threshold value that minimizes (7) from this range as the final threshold value.

$$\epsilon = \text{argmin}(\epsilon) = \frac{\sum_{i=1}^n (e_{an} - \epsilon)}{e_{an}} \quad (7)$$

$e_{an} = \{e \in \mathbf{e} \mid e > \epsilon\}$ , where  $n$  is the number of anomalous points.

The implementation steps of this method are shown in Algorithm 1.

Experiments show that in addition to quickly determining the detection threshold, this method can also correct the threshold in real time based on the detected alarm rate. The threshold correction strategy is as follows.

When performing anomaly detection, within the time window  $T$ , if the ratio of detected anomalies is not within  $P_1 \sim P_2$ , the threshold setting is considered to be unreasonable and needs to be corrected. The correction is made according to the method of automatically defining the threshold proposed in this paper, as Algorithm 2 shows.

##### C. ANOMALY PRUNING BASED ON CAUSALITY

False anomalies are a phenomenon that often occur in anomaly detection. In order to judge whether the detected anomaly is a real anomaly from the perspective of the system, we propose an improved multivariate transfer entropy algorithm to identify the causality between telemetry parameters. When an anomaly is detected, only the causal parameter of the parameter that is also anomalous can be regarded as a real anomaly; otherwise, it will be regarded as a false

**Algorithm 1** cal\_threshold

```

1: procedure cal_threshold( $e$ ,  $P_1$ ,  $P_2$ )
2:    $\epsilon_1 \leftarrow \text{cal}(P(e < \epsilon_1) \geq P_1)$ 
3:    $\epsilon_2 \leftarrow \text{cal}(P(e < \epsilon) \leq P_2)$ 
4:   for  $i$  in  $[\epsilon_1, \epsilon_2]$  do
5:      $judge \leftarrow 1000$ 
6:      $e_{an} \leftarrow 0$ 
7:      $acc \leftarrow 0$ 
8:      $final_\epsilon \leftarrow 0$ 
9:     for  $j$  in  $e$  do
10:      if  $e[j] > i$  then
11:         $e_{an} \leftarrow e_{an} + 1$ 
12:         $acc \leftarrow acc + (e[j] - i)$ 
13:      end if
14:    end for
15:    if  $\frac{acc}{e_{an}} < judge$  then
16:       $judge \leftarrow \frac{acc}{e_{an}}$ 
17:       $final_\epsilon \leftarrow i$ 
18:    end if
19:  end for
20: end procedure

```

**Algorithm 2** update\_threshold

```

1: procedure update_threshold( $e$ ,  $\epsilon$ ,  $P_1$ ,  $P_2$ )
2:    $anomalies \leftarrow 0$ 
3:   for  $i$  in  $e$  do
4:      $judge \leftarrow 1000$ 
5:      $e_{an} \leftarrow 0$ 
6:      $acc \leftarrow 0$ 
7:      $final_\epsilon \leftarrow 0$ 
8:     if  $e[i] > \epsilon$  then
9:        $anomalies \leftarrow anomalies + 1$ 
10:       $final_\epsilon \leftarrow i$ 
11:    end if
12:  end for
13:  if  $P_1 \leq (anomalies / \text{len}(e)) \leq P_2$  then
14:     $final_\epsilon \leftarrow \epsilon$ 
15:  else
16:     $final_\epsilon \leftarrow \text{cal}_\text{thresold}(e, P_1, P_2)$ 
17:  end if
18: end procedure

```

anomaly. The specific anomaly pruning steps are shown in Algorithm 3.

**V. EXPERIMENTS****A. INTRODUCTION OF DATASET**

To verify the effectiveness of the method in this paper, we take the telemetry data of 17 parameters of a star (denoted as the A star), identify the causality, establish a GRU model for each parameter, and perform anomaly detection based on the actual telemetry data. The relevant data are described in Table 1. Fig.2 shows the data of some telemetry parameters. IN7, VN2, and TN10 are the telemetry data of the current,

**Algorithm 3** prun\_fpr

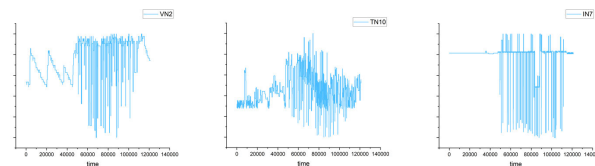
```

1: procedure prun_fpr( $z\_label$ ,  $x\_label$ )
2:   for  $i$  in  $x\_label$  do
3:     if  $x\_label[i] = 1$  then
4:       if  $z\_label[i] = 0$  then
5:          $x\_label[i] \leftarrow 0$ 
6:       end if
7:     end if
8:   end for
9: end procedure

```

**TABLE 1.** Telemetry data information of the A satellite.

| Attribute                      | Value    |
|--------------------------------|----------|
| number of telemetry parameters | 17       |
| data sampling duration         | 168 days |
| data sampling frequency        | 1 minute |
| length of each parameter       | 121168   |

**FIGURE 2.** Example of telemetry data.

voltage, and temperature, respectively, which contain anomalous states. The figure shows not only that there is not only a large amount of telemetry data but that the data also change irregularly, and it is difficult to model the data using general methods.

The parameter settings of the GRU model used in this paper are shown in Table 2. The GRU model includes two hidden layers, and each layer includes 128 units.

**TABLE 2.** Model parameters.

| Parameter             | Values |
|-----------------------|--------|
| hidden layers         | 2      |
| units in hidden layer | 0.1    |
| time steps            | 20     |
| batch size            | 256    |
| epoch                 | 100    |
| optimizer             | Adam   |

**B. EXPERIMENT 1: CAUSALITY IDENTIFICATION**

Using the original and improved multivariate transfer entropy methods, the causality of the 17 parameters of the A Star was identified. The results are shown in Table 3, Table 4 and Fig.3. The tables and figure show that there is a significant difference between the results of the improved method in Fig.3(b) and the original method in Fig.3(a). In general,

**TABLE 3. Telemetry Parameters Causality Table of the A satellite (the Original Multivariate Transfer Entropy).**

| Cause Parameters           | Parameter |
|----------------------------|-----------|
| Psan, VN2, IN3, TN9        |           |
| TG2, TG3, TK2, TK26        | Psas      |
| Psas, TN9, TG3, TK25, TK26 | Psan      |
| IN2, IN3, IN7, TN10, TK25  | VN2       |
| Psan, VN2, IN2, IN3, IN7   | VN10      |
| VN10, IN3, TN9, TN10, TG2  | IN2       |
| VN2                        | IN3       |
| IN3                        | IN7       |
| IN3, TK2                   | TN9       |
| Psas, VN2, IN2, IN3        | TN10      |
| TK8, TK2, TK25             | TG1       |
| TG1, TG3, TK9              | TG2       |
| TG2, TK8, TK2              | TG3       |
| TN9, TK9, TK2, TK25        | TK8       |
| Psas                       | TK9       |
| TK25, TK26                 | TK2       |
| IN2, IN7, TK25             | TK26      |

**TABLE 4. Telemetry Parameters Causality Table of the A satellite (the Improved Multivariate Transfer Entropy).**

| Cause Parameters    | Parameter |
|---------------------|-----------|
| IN3, IN7            | VN2       |
| Psan, IN2, IN3, IN7 | VN10      |
| IN3, TK2            | TN9       |
| Psas, VN2, IN2, IN3 | TN10      |
| Psas                | TK9       |
| IN2, IN7            | TK26      |

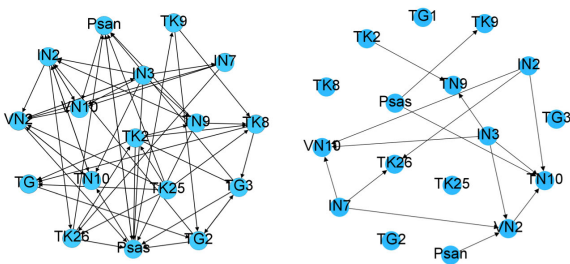


**FIGURE 3. Causality network.**left: (a) The Original Method right: (b) The Improved Method Causality network.

the improved multivariate transfer entropy method obtains fewer causal relationships, and there are no mutually causal parameters.

The analysis shows that it is sometimes difficult to obtain the effective causality using the original method, and the results are sometimes obviously incorrect. For example, Psan and Psas are the two parameters of the solar array output power. There is no causal relationship, but there is a very strong correlation. The original multivariate transfer entropy

method recognizes this correlation as mutual causality, which is inconsistent with the facts. The reason for this is that Psan and Psas are highly correlated, so the transfer entropy between the two are not considerably different. In the original multivariate transfer entropy method, both can pass the causality test, which leads to the phenomenon of mutual causality. However, their directional transfer entropy is small, so the causal relationship existing between them can be eliminated accordingly. This shows that only when the information flow of one parameter to another parameter is much larger than the information flow of another parameter to this parameter can it be reasonably considered that there is a causal relationship between these two parameters.

**C. EXPERIMENT 2: ANOMALY DETECTION AND PRUNING**

After dynamically defining the threshold and marking the points above the threshold as anomalous, we pruned the anomalies through the causal relationship between the telemetry parameters. Identifying the causal relationships shows that VN2 is the causal parameter of TN10. Therefore, when there is an anomaly in TN10 but no anomaly in VN2, it is regarded as a false anomaly and needs to be pruned. When an anomaly occurs in TN10, VN2 is also anomalous, and it is regarded as a real anomaly, as shown in Fig.4.

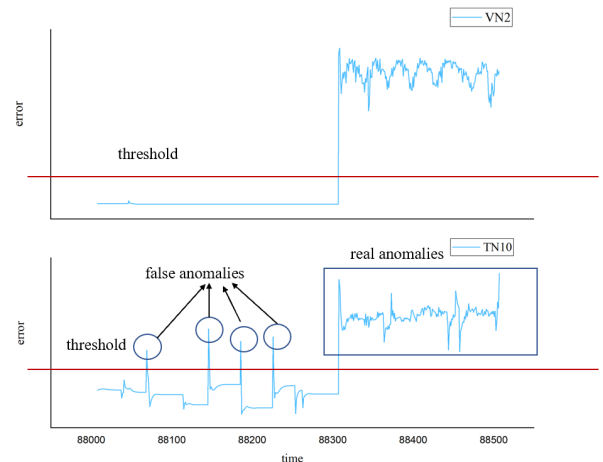


**FIGURE 4. Anomaly detection and pruning example.**

**D. EXPERIMENT 3: THRESHOLD CORRECTION**

To verify the effectiveness of the threshold correction method proposed in this paper, the threshold correction process in a certain period of time for parameter TN10 is selected for an illustration, as shown in Fig.5. In this experiment,  $T = 500$  because in the process of sampling telemetry data, the sampling frequency is 1 minute, and  $T = 500$  is approximately 8 hours to update the threshold. During the experiment, it is found that updating the threshold every 8 hours is a reasonable choice; if the interval is too short or too long, the detection effect will not be very good. In the time period from 1 to 500, because the initial threshold leads to a

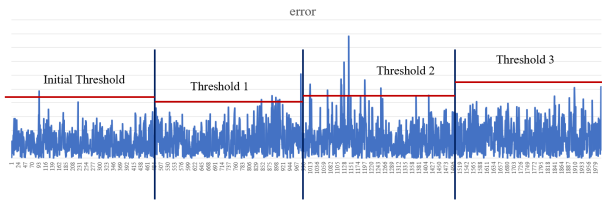


FIGURE 5. Threshold correction example.

TABLE 5. Comparison of Anomaly Detection Results.

|                 | precision     | recall   | F1-score      | FPR      |
|-----------------|---------------|----------|---------------|----------|
| GRU(pruning)    | <b>0.9041</b> | <b>1</b> | <b>0.9496</b> | <b>0</b> |
| GRU(no pruning) | 0.8978        | 0.9322   | 0.9147        | 0.0678   |
| LSTM-NDT[15]    | 0.8996        | 0.9966   | 0.9457        | 0.0034   |
| DSPOT[30]       | 0.8984        | 0.9294   | 0.9137        | 0.0706   |

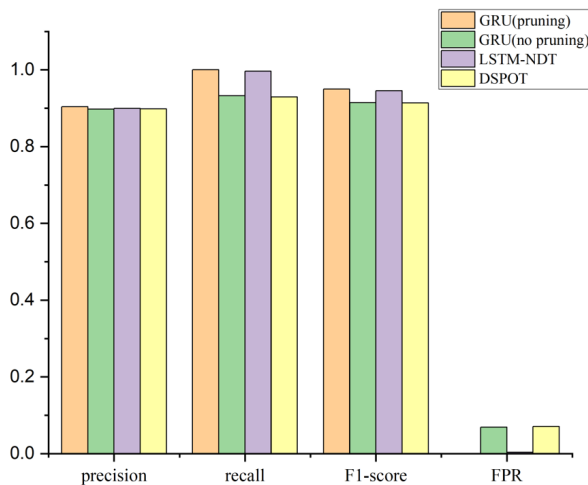


FIGURE 6. Performance comparison.

low false alarm rate, the threshold needs to be further reduced in the next time window to obtain Threshold 1. Furthermore, Threshold 1 causes the false alarm rate within the time period of 501-1000 to be too high, so the threshold needs to be modified to obtain Threshold 2. Threshold 2 causes the alarm rate to be too high, so it is necessary to increase the threshold to obtain Threshold 3. This process proves the effectiveness of the threshold correction method proposed in this paper.

#### E. EXPERIMENT 4: ALGORITHM PERFORMANCE COMPARISON

The comparison between the performance of this method and that of other methods is shown in Table 5 and Fig.6. The evaluation indicators are defined as follows:

$$\begin{aligned} \text{precision} &= \frac{TP}{TP + FP} \\ \text{recall} &= \frac{TP}{TP + FN} \\ \text{FPR} &= \frac{FN}{FN + TP} \end{aligned}$$

Table 5 and Fig.6 show that compared with other methods, the precision, recall, F1-score and FPR of the method proposed in this paper are improved compared with those of other typical methods. In particular, the FPR dropped significantly, which illustrates that the causality-based anomaly pruning strategy can greatly reduce the false positive rate and reduce the cost of anomaly detection.

After experimental verification, when modelling telemetry data using the GRU for training, the average training time of each epoch is 15.6 s, while the average training time of each epoch of classic LSTM is 35.8 s, and the training time of the GRU is obviously much shorter than that of the LSTM model; therefore, the GRU is more suitable for telemetry data modelling.

#### VI. CONCLUSION

This paper proposes a satellite on-orbit anomaly detection method based on automatically defined thresholds and causality pruning, and the results verify that the GRU model can predict telemetry data more accurately than the existing typical models. In addition, this paper proposes a method to automatically define the detection threshold based on the false positive rate. This method does not need to possess any prior knowledge about the data; it can define the appropriate detection threshold, and it includes a threshold correction strategy. This paper proposes a method of identifying the causal relationships between telemetry parameters and uses the causal relationships between them to carry out anomaly pruning. Compared with those of other methods, the recall and precision of this method are improved, and the false positive rate is significantly reduced.

The shortcoming of the single-channel GRU model is that it is not sufficiently sensitive to anomalies. When an anomaly occurs, the prediction performance of the normal state is poor, resulting in a small prediction residual under an abnormal state. In future research work, new models will be considered to improve the performance of model predictions and the sensitivity of the model to anomalies, and we will consider adding causal features to the predictive model to improve the model's sensitivity to anomalies.

#### REFERENCES

- [1] D. Agarwal, "An empirical Bayes approach to detect anomalies in dynamic multidimensional arrays," in *Proc. 5th IEEE Int. Conf. Data Mining (ICDM)*, Nov. 2005, pp. 26–33.
- [2] A. Barrett, "Model compilation for real-time planning and diagnosis with feedback," in *Proc. 19th Int. Joint Conf. Artif. Intell. (IJCAI)*, 2005, pp. 1195–1200.
- [3] Y. Chen, G. Rangarajan, J. Feng, and M. Ding, "Analyzing multiple nonlinear time series with extended Granger causality," *Phys. Lett. A*, vol. 324, no. 1, pp. 26–35, Apr. 2004.
- [4] K. Cho, B. van Merriënboer, C. Gulcehre, D. Bahdanau, F. Bougares, H. Schwenk, and Y. Bengio, "Learning phrase representations using RNN encoder–decoder for statistical machine translation," in *Proc. Conf. Empirical Methods Natural Lang. Process. (EMNLP)*, 2014, pp. 1724–1734.
- [5] J. Chung, C. Gulcehre, K. Cho, and Y. Bengio, "Empirical evaluation of gated recurrent neural networks on sequence modeling," 2014, *arXiv:1412.3555*. [Online]. Available: <http://arxiv.org/abs/1412.3555>
- [6] T. Ergen and S. S. Kozat, "Unsupervised anomaly detection with LSTM neural networks," *IEEE Trans. Neural Netw. Learn. Syst.*, vol. 31, no. 8, pp. 3127–3141, Aug. 2020.

- [7] E. Eskin, "Anomaly detection over noisy data using learned probability distributions," in *Proc. 17th Int. Conf. Mach. Learn. (ICML)*, 2000, pp. 255–262.
- [8] J. Geweke, "Measurement of linear dependence and feedback between multiple time series," *J. Amer. Stat. Assoc.*, vol. 77, no. 378, pp. 304–313, Jun. 1982.
- [9] C. Granger, "Investigating causal relations by econometric models and cross-spectral methods," *Econometrica*, vol. 37, no. 3, pp. 424–438, 1969.
- [10] F. Guigou, P. Collet, and P. Parrend, "SCHEDA: Lightweight Euclidean-like heuristics for anomaly detection in periodic time series," *Appl. Soft Comput.*, vol. 82, Sep. 2019, Art. no. 105594.
- [11] L. Haan and A. Ferreira, "Extreme value theory: An introduction," *Ser. Oper. Res. Financial Eng.*, vol. 60, no. 1, pp. 1–20, 2006.
- [12] S. Hochreiter and J. Schmidhuber, "Long short-term memory," *Neural Comput.*, vol. 9, no. 8, pp. 1735–1780, 1997.
- [13] X. Hu, H. Zhang, D. Ma, and R. Wang, "A tGAN-based leak detection method for pipeline network considering incomplete sensor data," *IEEE Trans. Instrum. Meas.*, vol. 70, pp. 1–10, 2021.
- [14] P.-S. Huang, F. Fahmi, and F.-J. Wang, "Improving the detection of artifact anomalies in a workflow analysis," *IEEE Trans. Rel.*, vol. 70, no. 2, pp. 692–710, Jun. 2021.
- [15] K. Hundman, V. Constantinou, C. Laporte, I. Colwell, and T. Soderstrom, "Detecting spacecraft anomalies using LSTMs and nonparametric dynamic thresholding," in *Proc. 24th ACM SIGKDD Int. Conf. Knowl. Discovery Data Mining*, Jul. 2018, pp. 387–395.
- [16] R. E. Kalman and R. S. Bucy, "New results in linear filtering and prediction theory," *J. Basic Eng.*, vol. 83, no. 1, pp. 95–108, Mar. 1961.
- [17] T. Kim and C. H. Park, "Anomaly pattern detection for streaming data," *Expert Syst. Appl.*, vol. 149, Jul. 2020, Art. no. 113252.
- [18] R. Laxhammar and G. Falkman, "Online learning and sequential anomaly detection in trajectories," *IEEE Trans. Pattern Anal. Mach. Intell.*, vol. 36, no. 6, pp. 1158–1173, Jun. 2014.
- [19] D. Li, D. Chen, B. Jin, L. Shi, J. Goh, and S.-K. Ng, "MAD-GAN: Multivariate anomaly detection for time series data with generative adversarial networks," in *Proc. Int. Conf. Artif. Neural Netw.*, 2019, pp. 703–716.
- [20] B. Lindner, L. Auret, and M. Bauer, "A systematic workflow for oscillation diagnosis using transfer entropy," *IEEE Trans. Control Syst. Technol.*, vol. 28, no. 3, pp. 908–919, May 2020.
- [21] J. Lizier and M. Rubinov, "Multivariate construction of effective computational networks from observational data," *Avian Diseases*, vol. 30, no. 1, pp. 1–2, 2012.
- [22] R. Marschinski and H. Kantz, "Analysing the information flow between financial time series: An improved estimator for transfer entropy," *Eur. Phys. J. B*, vol. 30, no. 2, pp. 275–281, Nov. 2002.
- [23] B. Nachman and D. Shih, "Anomaly detection with density estimation," *Phys. Rev. D, Part. Fields*, vol. 101, no. 7, p. 75042, Apr. 2020.
- [24] S. Narasimhan and L. Brownston, "HyDE framework for stochastic and hybrid model-based diagnosis," *NASA Tech Briefs*, vol. 36, no. 4, p. 59, 2012.
- [25] L. Novelli, P. Wollstadt, P. Mediano, M. Wibral, and J. T. Lizier, "Large-scale directed network inference with multivariate transfer entropy and hierarchical statistical testing," *Netw. Neurosci.*, vol. 3, no. 3, pp. 827–847, Jan. 2019.
- [26] M. Odiathevar, W. K. G. Seah, M. Frean, and A. Valera, "An online offline framework for anomaly scoring and detecting new traffic in network streams," *IEEE Trans. Knowl. Data Eng.*, early access, Jan. 11, 2021, doi: 10.1109/TKDE.2021.3050400.
- [27] E. A. Omran and W. A. Murtada, "Efficient anomaly classification for spacecraft reaction wheels," *Neural Comput. Appl.*, vol. 31, no. 7, pp. 2741–2747, Jul. 2019.
- [28] B. Pilastre, L. Boussoif, S. D'Escrivan, and J.-Y. Tourneret, "Anomaly detection in mixed telemetry data using a sparse representation and dictionary learning," *Signal Process.*, vol. 168, Mar. 2020, Art. no. 107320.
- [29] T. Schreiber, "Measuring information transfer," *Phys. Rev. Lett.*, vol. 85, no. 2, pp. 461–464, Jul. 2000.
- [30] A. Siffer, P.-A. Fouque, A. Termier, and C. Largouet, "Anomaly detection in streams with extreme value theory," in *Proc. 23rd ACM SIGKDD Int. Conf. Knowl. Discovery Data Mining*, Aug. 2017, pp. 1067–1075.
- [31] L. Song, T. Zheng, J. Wang, and L. Guo, "An improvement growing neural gas method for online anomaly detection of aerospace payloads," *Soft Comput.*, vol. 24, no. 15, pp. 11393–11405, Aug. 2020.
- [32] S. Tariq, S. Lee, Y. Shin, M. S. Lee, O. Jung, D. Chung, and S. S. Woo, "Detecting anomalies in space using multivariate convolutional LSTM with mixtures of probabilistic PCA," in *Proc. 25th ACM SIGKDD Int. Conf. Knowl. Discovery Data Mining*, Jul. 2019, pp. 2123–2133.
- [33] R. Vicente, M. Wibral, M. Lindner, and G. Pipa, "Transfer entropy—A model-free measure of effective connectivity for the neurosciences," *J. Comput. Neurosci.*, vol. 30, no. 1, pp. 45–67, Feb. 2011.
- [34] R. Wang, Q. Sun, W. Hu, J. Xiao, H. Zhang, and P. Wang, "Stability-oriented droop coefficients region identification for inverters within weak grid: An impedance-based approach," *IEEE Trans. Syst., Man, Cybern. Syst.*, vol. 51, no. 4, pp. 2258–2268, Apr. 2021.
- [35] W. Wang, F. Chang, and H. Mi, "Intermediate fused network with multiple timescales for anomaly detection," *Neurocomputing*, vol. 433, pp. 37–49, Apr. 2021.
- [36] B. C. Williams, M. D. Ingham, S. Chung, P. Elliott, M. Hofbauer, and G. T. Sullivan, "Model-based programming of fault-aware systems," *AI Mag.*, vol. 24, no. 4, pp. 61–75, 2004.
- [37] J. Wu, L. Yao, B. Liu, Z. Ding, and L. Zhang, "Combining OC-SVMs with LSTM for detecting anomalies in telemetry data with irregular intervals," *IEEE Access*, vol. 8, pp. 106648–106659, 2020.
- [38] Y. K. Takehisa Yairi, "Telemetry-mining: A machine learning approach to anomaly detection and fault diagnosis for space systems," in *Proc. 2nd IEEE Int. Conf. Space Mission Challenges Inf. Technol. (SMC-IT)*, 2006, pp. 466–476.
- [39] M. Yu and S. Sun, "Policy-based reinforcement learning for time series anomaly detection," *Eng. Appl. Artif. Intell.*, vol. 95, Oct. 2020, Art. no. 103919.



**SIYA CHEN** received the B.Eng. degree in information management and information system from Jilin University, Changchun, China, in 2019. She is currently pursuing the M.Sc. degree in management science and engineering with the National University of Defense Technology, Changsha, China. Her research interests include spacecraft fault diagnosis and anomaly detection.



**JIN G.** was born in Hebei, China. He received the Ph.D. degree from the National University of Defense Technology, Changsha, China, in 2000. He is currently a Professor with the School of System Engineering, National University of Defense Technology. His research interests include health management and system test and evaluation.



**XINYU MA** received the M.Sc. degree in management science and engineering from the National University of Defense Technology, Changsha, China, in 2019. She is currently an Engineer with the Beijing Aerospace Control Center.